



## Bortezomib Alone and in Combination With Salinosporamid A Induces Apoptosis and Promotes Pheochromocytoma Cell Death *In Vitro* and in Female Nude Mice

Petra Bullova,<sup>1,2\*</sup> Antony Cougnoux,<sup>3\*</sup> Geena Marzouca,<sup>1</sup> Juraj Kopacek,<sup>2</sup> and Karel Pacak<sup>1</sup>

<sup>1</sup>Section on Medical Neuroendocrinology, Eunice Kennedy Shriver National Institute of Child Health and Human Development, National Institutes of Health, Bethesda, Maryland 20892; <sup>2</sup>Department of Molecular Medicine, Institute of Virology, Biomedical Research Center, Slovak Academy of Sciences, 84505 Bratislava, Slovakia; and <sup>3</sup>Section on Molecular Dismorphology, Eunice Kennedy Shriver National Institute of Child Health and Human Development, National Institutes of Health, Bethesda, Maryland 20892

Proteasome inhibitors have been frequently used in treating hematologic and solid tumors. They are administered individually or in combination with other regimens, to prevent severe side effects and resistance development. Because they have been shown to be efficient and are pharmaceutically available, we tested the first Food and Drug Administration–approved proteasome inhibitor bortezomib alone and in combination with another proteasome inhibitor, salinosporamid A, in pheochromocytoma cells. Pheochromocytomas/Paragangliomas (PHEOs/PGLs) are neuroendocrine tumors for which no definite cure is yet available. Therefore, drugs with a wide spectrum of mechanisms of action are being tested to identify suitable candidates for PHEO/PGL treatment. In the current study, we show that bortezomib induces PHEO cell death via the apoptotic pathway *in vitro* and *in vivo*. The combination of bortezomib with salinosporamid A exhibits additive effect on these cells and inhibits proliferation, cell migration and invasion, and angiogenesis more potently than bortezomib alone. Altogether, we suggest these proteasome inhibitors, especially bortezomib, could be potentially tested in PHEO/PGL patients who might benefit from treatment with either the inhibitors alone or in combination with other treatment options. (*Endocrinology* 158: 3097–3108, 2017)

Targeted therapy is an emerging treatment option for various types of cancer, not only because of its efficacy, but also because of its preferential effect on cancer cells. Moreover, it is generally better tolerated by patients than other therapies (*i.e.*, chemotherapy) (1). One of the main disadvantages, similar to other options, however, is the development of tumor cell resistance appearing soon after beginning the treatment; therefore, combinations of two or more compounds are often desirable (2).

Proteasome inhibitors are a group of compounds that have become frequently used in cancer therapy (3).

The 26S mammalian proteasome is a multiprotein enzymatic complex composed of the 20S core particle and two 19S regulatory particles (4). It is the final player in the ubiquitin–proteasome pathway, resulting in degradation of proteins. The proteasome recognizes proteins marked with ubiquitin for degradation, and thus regulates the strictly controlled cell protein balance under normal conditions. The 20S subunit contains three different enzymatic domains exerting specific catalytic activities—chymotrypsin-like, trypsin-like, and caspase-like—which are the primary targets for proteasome inhibitors (3).

ISSN Print 0013-7227 ISSN Online 1945-7170

Printed in USA

Received 26 June 2017. Accepted 9 August 2017.

First Published Online 15 August 2017

\*These authors contributed equally to this work.

Abbreviations: CVD, cyclophosphamide, vincristine, and dacarbazine; EMT, epithelial–mesenchymal transition; MPC, mouse pheochromocytoma cell; mRNA, messenger RNA; MTT, mouse tumor tissue; NF- $\kappa$ B, nuclear factor- $\kappa$ B; PARP, poly(ADP-ribose) polymerase; PHEO/PGL, pheochromocytoma/paraganglioma; RRID, Research Resource Identifier; SDHB, succinate dehydrogenase complex iron sulfur subunit B.

The first-in-class proteasome inhibitor that was approved by the Food and Drug Administration is bortezomib (Velcade). It reversibly binds to threonine residues in the active site of the chymotrypsin-like catalytic region of the 20S subunit and thus inhibits its function (5). In initial studies, bortezomib showed efficacy in the treatment of various types of cancer, including multiple myeloma, mantle cell lymphoma, prostate, colon, and pancreatic cancer (5). It activates several signaling pathways leading to cell death, including apoptosis and autophagy, and it is also known to block the nuclear factor- $\kappa$ B (NF- $\kappa$ B) pathway, thus sensitizing cancer cells to chemotherapy and increasing their susceptibility to apoptotic cell death (5, 6). Bortezomib has also proven to be effective in combination with other proteasome inhibitors, chemotherapeutic agents, or radiation therapy (3, 7). Following the success of bortezomib in antitumor therapies, second-generation proteasome inhibitors, including carfilzomib, ixazomib, delanzomib, oprosomib, and salinosporamid A, were developed, also exhibiting promising results (8, 9).

Salinosporamid A (NPI-0052, marizomib) is a proteasome inhibitor originally isolated from the marine organism *Salinospora tropica* (10). It has been shown to be effective at inducing cell death in several cancer cell lines *in vitro* and *in vivo*, either as a single treatment or in combination with other compounds (10). It has been very frequently compared with bortezomib, with some studies showing that salinosporamid A was more effective and exhibited less side effects (8). Unlike bortezomib, salinosporamid A binds irreversibly to the active sites of all three catalytic regions of the 20S subunit (10). Salinosporamid A has been tested, either alone or in combination, in clinical trials for several cancers, including relapsed or refractory multiple myeloma and malignant glioma (11, 12).

Pheochromocytomas/Paragangliomas (PHEOs/PGLs) are rare neuroendocrine tumors that lack curative therapy for metastatic disease. The only effective treatment other than surgery is a combination of cyclophosphamide, vincristine, and dacarbazine (CVD); however, resistance is acquired in most patients (13). Like in other types of cancer, several compounds have been tested in PHEO/PGL in the search for effective treatment (14), including topoisomerase (15), mTOR pathway (16), heat-shock protein 90 (17), and tyrosine kinase (18) inhibitors. The results obtained with these drugs *in vitro* and in animal models showed rationale for testing them in clinical trials for PHEO/PGL.

In the present work, we studied the effects of bortezomib and salinosporamid A independently and in combination on two established PHEO cell lines, mouse pheochromocytoma cells (MPC) and mouse tumor tissue (MTT) cells (14). We found that both compounds are effective in these cells, although salinosporamid A is less

effective in individual treatment both *in vitro* and *in vivo*. Both drugs exert their activity on the cells via induction of apoptosis and inhibition of migration and invasion *in vitro*, and bortezomib and the combination delayed tumor growth in animal models. Moreover, in *in vivo* studies, tumor growth inhibition with a combination of both drugs at lower doses was comparable to bortezomib alone at a higher dose. The combination also showed an additive inhibitory effect on PHEO cell proliferation, migration, invasion, and apoptosis induction *in vitro* and *in vivo*. In conclusion, we propose that bortezomib is a potential candidate for treatment of PHEO/PGL, especially as a part of a combination therapy. Furthermore, addition of salinosporamid A might allow to reduce bortezomib doses, possibly resulting in fewer side effects and a lower risk of resistance development.

## Materials and Methods

### Cell lines and reagents

The mouse pheochromocytoma cell lines MPC, MTT, and MTT-Luc (19) were maintained in Dulbecco's modified Eagle medium supplemented with 10% fetal bovine serum, 5% horse serum, and antibiotic/antimycotic (Life Technologies, Carlsbad, CA). Bortezomib was purchased from Selleckchem (Houston, TX), and salinosporamid A from Adipogen (San Diego, CA); stock solutions were stored at  $-20^{\circ}\text{C}$  and thawed prior to use.

### Cell viability assay

Cell viability was assessed by the ability of cells to metabolize methylthiazolyldiphenyl-tetrazolium bromide (Sigma-Aldrich, St. Louis, MO), according to the manufacturer's instructions. Cells were seeded onto 96-well plates (Corning Inc., Corning, NY) at  $1.0 \times 10^4$  cells/well and maintained at  $37^{\circ}\text{C}$  overnight prior to the initiation of experimental treatments. The cells were treated with 0, 1, 10, 100, and 1000 nM bortezomib or salinosporamid A for 48 hours; in combination treatments, 10 nM salinosporamid A was combined with 1, 10, 100, and 1000 nM bortezomib. Following the indicated treatments, 10  $\mu\text{L}$  methylthiazolyldiphenyl-tetrazolium bromide solution at 5 mg/mL was added to each well, and the cells were maintained in growth medium for 3 hours at  $37^{\circ}\text{C}$ . The cells were lysed, and absorbance at 490 nm was subsequently measured using a spectrophotometer (Omega Scientific, Offenburg, Germany). Untreated cells were used as controls. Cell viability was calculated as a percentage compared with untreated controls, and  $\text{LD}_{50}$ , the dose leading to the death of 50% of the cells, was determined.

### Cell migration and invasion assay

For the migration assay, an MPC suspension was prepared at a concentration of  $0.5 \times 10^6$  cells/mL in serum-free medium with or without tested drug. A total of 300  $\mu\text{L}$  suspension was added to Transwell chambers with 8- $\mu\text{m}$  pores (BD Biosciences, San Diego, CA), which were placed in 24-well plates with 500  $\mu\text{L}$  complete medium per well, with or without tested drug. The treatments were as follows: 1 nM bortezomib, 10 nM salinosporamid A, and the combination of 1 nM bortezomib

with 10 nM salinosporamid A. The cells were allowed to migrate for 24 hours. At the end of the experiment, nonmigrated cells from the upper parts of the chambers were removed with cotton swabs, and migrated cells were fixed in methanol and stained with 4',6-diamidino-2-phenylindole (Life Technologies). The number of migrated cells was assessed using fluorescence microscope and analyzed with ImageJ software (National Institutes of Health, Bethesda, MD). The invasion assay was performed the same way using matrigel-coated Transwell chambers (Corning Inc.).

### Western blotting

The cells were washed twice with ice-cold phosphate-buffered saline and lysed in radioimmunoprecipitation assay buffer (Cell Signaling Technology, Danvers, MA) supplemented with Complete protease inhibitor cocktail (Roche, Basel, Switzerland) and phosphatase inhibitor cocktail (Cell Signaling Technology). Protein lysates were denatured and separated by 4% to 12% NuPAGE Bis-Tris gel (Life Technologies) and transferred to polyvinylidene difluoride membrane (Bio-Rad Laboratories, Hercules, CA). The membrane was incubated with primary antibodies overnight at 4°C, followed by incubation with the corresponding horseradish peroxidase-conjugated secondary antibody [Research Resource Identifier (RRID): AB\_772209; RRID: AB\_772206; GE Health Care Life Sciences, Pittsburgh, PA] at room temperature for 1 hour. The Western blots were visualized using Thermo Scientific ECL Plus reagent (Thermo Scientific Inc., Pittsburgh, PA). Densitometric analysis was performed using LabImage 4.1 (Bio-Rad Laboratories). The primary antibodies used included anti-cleaved caspase 3 (RRID: AB\_2070042), anti-caspase 3 (RRID: AB\_2069872), anti-cleaved poly(ADP-ribose) polymerase (PARP) (RRID: AB\_2160592), and anti-ubiquitin (RRID: AB\_2180538) (Cell Signaling Technology), and anti- $\beta$ -tubulin (RRID: AB\_1844090) (Sigma-Aldrich).

### RNA extraction and real-time quantitative polymerase chain reaction

Messenger RNA (mRNA) was extracted using the RNAQuick-micro kit (Zymo Research, Irvine, CA). mRNA was quantified by Nanodrop (Thermo Scientific Inc.), and 1  $\mu$ g was reverse transcribed with the SuperScript III RT kit (Life Technologies), according to the manufacturer's instructions. Quantitative polymerase chain reaction was performed in ABI Vii7 (Life Technologies) using TaqMan probes for *Snail1*, *Snail2*, *Twist1*, *Nanog*, *Epo*, and *Vegfa* (Life Technologies). The amount of mRNA detected was normalized to control *Actb* mRNA values. Relative gene expression was calculated as a percentage of the value obtained in nontreated animals from the same experiment.

### Animal experiments and bioluminescence imaging

All animal studies were conducted in accordance with the principles and procedures outlined in the National Institutes of Health *Guide for the Care and Use of Animals* and approved by the National Institutes of Health Animal Care and Use Committee. A total of  $1.5 \times 10^6$  MTT-Luc cells was injected subcutaneously in the right lower dorsal side of female athymic nude mice (Charles River, Germantown, MD). The experimental groups consisted of 6-week-old mice housed in a pathogen-free facility. After 10 days, allowing for tumor cells to engraft, we started intraperitoneal injection with bortezomib (1 mg/kg;  $n = 10$ ), salinosporamid A (0.075 mg/kg;

$n = 10$ ), or the combination (0.25 mg/kg + 0.025 mg/kg salinosporamid A;  $n = 10$ ) twice per week for 28 days. Each group also had control animals treated with vehicle ( $n = 10$  per experiment). The animals were imaged weekly by bioluminescence. All bioluminescent data were collected with a Xenogen IVIS system (STTARR, Toronto, ON, Canada). For *in vivo* imaging, luciferase activity was assessed in anesthetized animals 10 minutes after intraperitoneal administration of 150 mg/kg luciferin (VivoGlo; Promega, Fitchburg, WI) in phosphate-buffered saline. The experiments were performed in the National Institutes of Health Mouse Image Facility in accordance with Animal Care and Use Committee regulations. All imaging variables were equal, and photographic and bioluminescent images at different time points were collected for each sample.

### Immunofluorescence staining and analysis

The tumors from the animals were embedded in paraffin, and slides with 5- $\mu$ m-thick tissue recuts were prepared. The tissue was deparaffinized and rehydrated prior to antigen retrieval in citrate sodium buffer (pH 6.0) for 20 minutes. The sections were incubated with primary antibody for 1 hour at room temperature, followed by 1-hour incubation with secondary antibody labeled with DyLight 594 (RRID: AB\_2336413) (Vector Laboratories, Burlingame, CA). The nuclei were labeled with NucBlue Live ReadyProbes Reagent (Life Technologies) for 10 minutes and mounted with Mowiol mounting solution (Millipore, Billerica, MA). The staining was analyzed by fluorescence microscopy. The primary antibodies used included anti-Ki67 (RRID: AB\_443209), anti-CD31 (RRID: AB\_726362) (Abcam, Cambridge, UK), and cleaved caspase 3 (RRID: AB\_2070042) (Cell Signaling Technology). All immunofluorescence staining was acquired by a Zeiss AxioObserver Z1 microscope fitted with an automated scanning stage, Colibri II LED illumination, and Zeiss ZEN software using a high-resolution AxioCam MRm camera and a 20 $\times$  objective. Each fluorophore channel was pseudo-colored in ZEN2 (Zeiss, Oberkochen, Germany), exported as TIFF, and analyzed using the FIJI distribution of ImageJ (20). Vessel length and density were measured from CD31-stained images. Vessel length was measured from stitched image covering the entire section. Vessel density corresponds to the percentage of the field stained for CD31. The proliferation index and cleaved caspase 3 ratio were determined by automatic counting of cell nuclei and positive staining. The ratio (positive signal/nuclei) was calculated in Excel (Microsoft, Redmond, WA). At least six images were used from each of the five tumors (per group) analyzed.

### Statistical analyses

Statistical analyses were performed using GraphPad Prism software to calculate the nonparametric Mann-Whitney *U* test (GraphPad Software, San Diego, CA).

## Results

### Bortezomib and salinosporamid A exhibit cytotoxic effect on mouse PHEO cells

To investigate the possible use of bortezomib and salinosporamid A in PHEO therapy, we first evaluated the cytotoxic effect of these compounds on mouse PHEO cells *in vitro*. MPC and MTT cells were treated with

bortezomib, salinosporamid A, or their combination. After 48 hours of incubation, the LD<sub>50</sub> was 7.3 nM and 6.3 nM for bortezomib and 107.2 nM and 42.43 nM for salinosporamid A in MPC and MTT cells, respectively, demonstrating a higher sensitivity of these cells to bortezomib than salinosporamid A [Fig. 1(a)]. To evaluate the cytotoxic effect of the bortezomib and salinosporamid A combination, MPC and MTT cells were treated with the concentrations described in Fig. 1(b). The addition of 10 nM salinosporamid A to both 10 nM and 100 nM bortezomib resulted in a significantly reduced number of viable MPC ( $P = 0.0015$  and  $P = 0.0390$ , respectively) and MTT ( $P = 0.0197$  and  $P < 0.0001$ , respectively) cells than when the same concentration of bortezomib was used alone, suggesting an additive effect on PHEO cells [Fig. 1(b)].

### Bortezomib and salinosporamid A decrease PHEO cell migration and invasion

Because migration and invasion are key processes in carcinogenesis, especially in metastasis development, we next evaluated the effect of the two proteasome inhibitors on migratory abilities of the cells. We treated MPC with bortezomib, salinosporamid A, and both in combination at sublethal doses. Although there was not a significant difference in migration of the cells treated with salinosporamid A, we observed a significantly decreased number of migrated cells treated with bortezomib when compared with control cells ( $P = 0.0043$ ) [Fig. 1(c)]. The combination of bortezomib and salinosporamid A further inhibited cell migration ( $P = 0.0022$ ). Similarly, bortezomib significantly inhibited invasion of MPC ( $P < 0.0001$ ), and this inhibition was magnified in combination with salinosporamid A ( $P < 0.0001$ ). Salinosporamid A did not significantly affect invasion of the cells when used as a single treatment. No cytotoxicity was observed at any of these drug concentrations. These results suggest that bortezomib alone or in combination with salinosporamid A is an effective inhibitor of migration and invasion of PHEO cells and might exhibit antimetastatic properties *in vivo*.

### Bortezomib and salinosporamid A exert their cytotoxic effect via apoptosis in PHEO cells *in vitro*

The ability of proteasome inhibitors to induce cell death via apoptosis has been well established (4). To investigate whether these drugs exhibited their cytotoxic effect via the same mechanism in PHEO cells, we treated MPC and MTT cells with bortezomib or salinosporamid A for 24 hours. As hypothesized, the treatments led to accumulation of ubiquitinated proteins in the PHEO cells. Although in bortezomib-treated cells the elevated level of ubiquitinated proteins was seen at 10 nM, a similar

effect in cells treated with salinosporamid A was not observed until 100 nM [Fig. 2(a)]. We also detected increased levels of the apoptotic markers cleaved caspase 3 and cleaved PARP in treated cells. Again, a 10-fold lower concentration of bortezomib was sufficient to induce a similar effect to the one seen in cells treated with 100 nM salinosporamid A. Based on the observed additive effect of the bortezomib and salinosporamid A combination, we treated MPC and MTT cells with 100 nM bortezomib, 100 nM salinosporamid A, and combinations of the two for 0, 8, 16, and 24 hours. The strongest induction of apoptosis was seen in cells treated with bortezomib alone at all time points, beginning at 8 hours. However, after 24 hours, the difference in the levels of cleaved caspase 3 and cleaved PARP between 100 nM bortezomib alone and the combination of 5 nM bortezomib and 10 nM salinosporamid A was less striking. At all time points, treatment with salinosporamid A alone induced the apoptotic pathway to the least extent [Fig. 2(b)]. These results suggest that bortezomib and salinosporamid A induce cell death through apoptosis and that 10 times lower concentrations of each compound in the combination are sufficient to produce a similar outcome.

### Combined bortezomib and salinosporamid A inhibits tumor growth of mouse PHEO

To test the effect of bortezomib and salinosporamid A *in vivo*, we divided the animals into three groups and treated them with bortezomib, salinosporamid A, or a combination of the two. After 21 days of treatment, we observed a significant inhibition of tumor growth in the animals treated with bortezomib alone ( $P = 0.0036$ ) and the combination ( $P = 0.0371$ ). The growth remained delayed until the end of the study at 28 days ( $P = 0.0068$ ,  $P = 0.0209$ , respectively). The tumors were also significantly smaller in the treated groups after 28 days of treatment [Fig. 3(a) and 3(b)]. We did not observe tumor growth inhibition in animals treated only with salinosporamid A.

Based on our *in vitro* results showing the inhibitory effect of the compounds on cell migration and invasion of MPC, we evaluated the gene expression of epithelial–mesenchymal transition (EMT), stem cell, and proangiogenic markers in the tumors. The expression levels of *Snail1*, *Snail2*, and *Twist1* were not significantly modified in any of the treatment groups when compared with control animals. In contrast, the expression levels of the proangiogenic factor *Epo* were significantly decreased in the animals treated with either individual drug or their combination [Fig. 3(c)]. Compared with controls, the  $P$  values were 0.0355, 0.0019, and 0.0002 for the bortezomib group, salinosporamid A group, and the combination group, respectively. *Vegfa* expression levels were significantly lower only in the group treated with the combination ( $P = 0.0011$ ). In addition, we

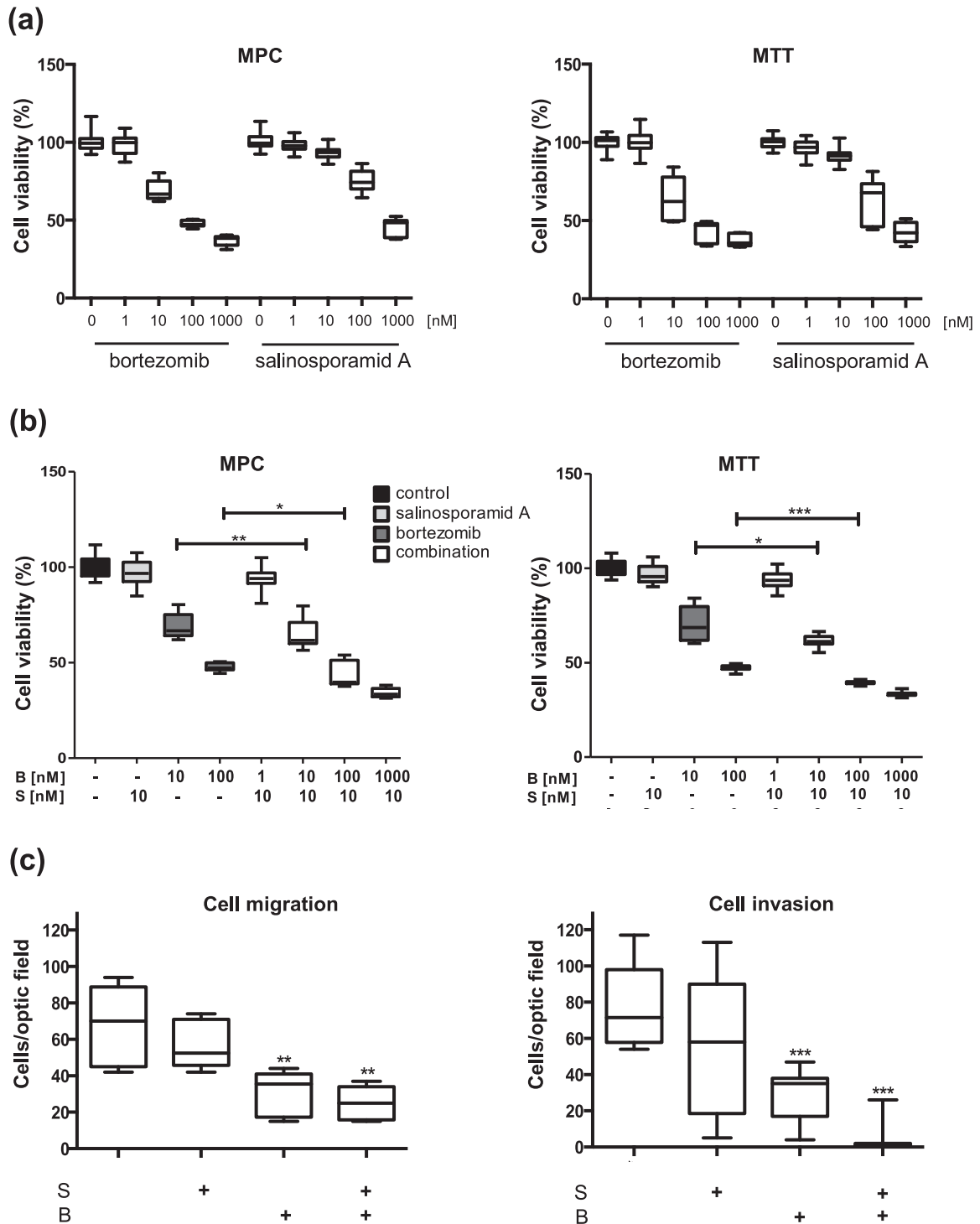


**Figure 1.** Bortezomib alone and in combination with salinosporamid A exhibits cytotoxic effect on PHEO cells and inhibits their migration and invasion. (a) MPC and MTT cells were treated with the indicated concentrations of bortezomib or salinosporamid A for 48 hours. Cell viability was assessed by methylthiazolyl-diphenyl-tetrazolium bromide assay. The box and whiskers graphs represent data from three independent experiments. (b) MPC and MTT cells were treated with the indicated concentrations of bortezomib, salinosporamid A, or their combination for 48 hours. Cell viability was assessed by methylthiazolyl-diphenyl-tetrazolium bromide assay. The box and whiskers graphs represent data from three independent experiments. (c) A total of  $1.5 \times 10^5$  MPC was plated in the upper part of Transwell chambers and allowed to migrate for 24 hours in the presence of bortezomib, salinosporamid A, or their combination. In the case of invasion, matrigel-coated Transwell chambers were used. The box and whiskers graph represents data from three independent experiments. \* $P < 0.05$ ; \*\* $P < 0.01$ ; \*\*\* $P < 0.001$ , Mann-Whitney  $U$  test. B, 1 nM bortezomib; S, 10 nM salinosporamid A.

detected significantly lower expression of the stem cell marker *Nanog* in the bortezomib ( $P = 0.0262$ )- and combination ( $P = 0.0004$ )-treated groups [Fig. 3(c)].

To assess the mechanism of action of the drugs in the allograft mouse models, sections were taken from control and treated tumors and stained for proliferation (Ki67),

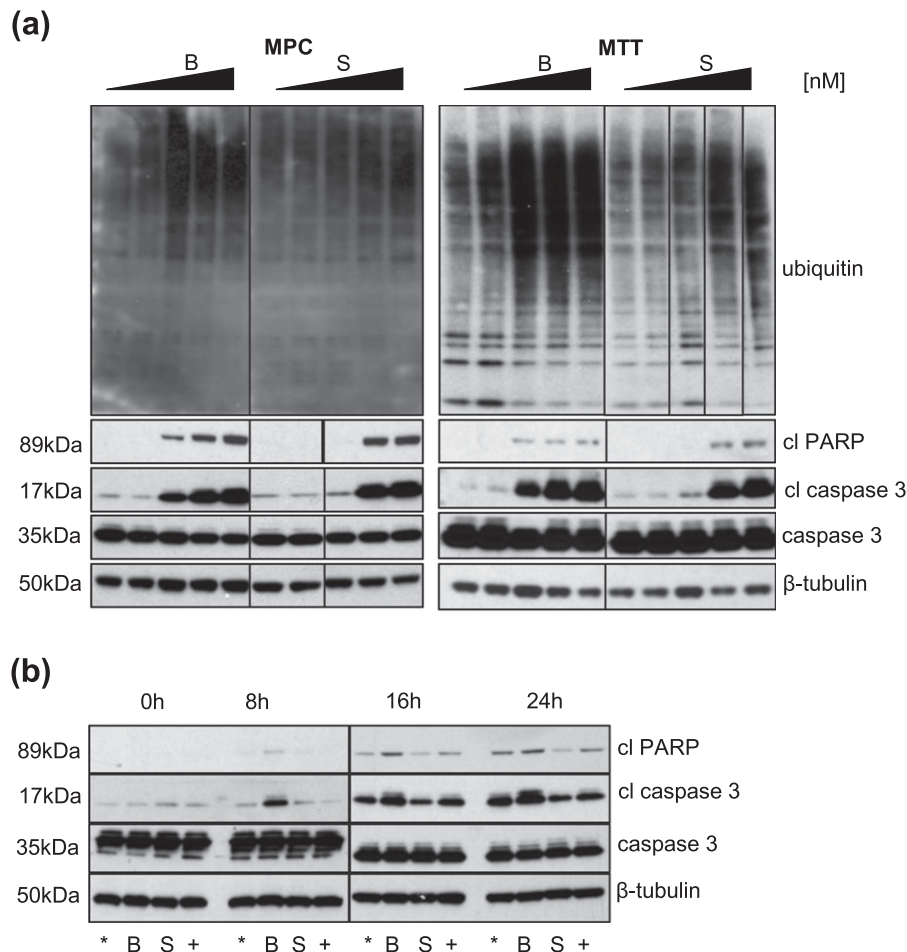


**Figure 2.** Bortezomib and salinosporamid A activate apoptosis in PHEO cells. (a) MPC and MTT cells were treated with bortezomib or salinosporamid A, at concentrations of 0, 1, 10, 100, and 1000 nM for 24 hours. Total cell lysates were subjected to Western blot with antibodies against ubiquitin, cleaved PARP, cleaved caspase 3, and caspase 3.  $\beta$ -tubulin was used as a loading control. A representative image ( $n = 3$ ) is shown. (b) MPC were treated with 100 nM bortezomib, 100 nM salinosporamid A, or their combination. Time course analysis of cleaved PARP, cleaved caspase 3, and caspase 3 in total cell lysates was performed.  $\beta$ -tubulin was used as a loading control. A representative image ( $n = 3$ ) is shown. \*, 10 nM salinosporamid A + 5 nM bortezomib; +, 10 nM salinosporamid A + 10 nM bortezomib; B, 100 nM bortezomib; S, 100 nM salinosporamid A.

angiogenesis (CD31), and apoptosis (cleaved caspase 3) markers. When compared with the control mice, proliferation was significantly inhibited in tumors treated with bortezomib and the combination ( $P = 0.0016$ ,  $P < 0.0001$ , respectively), whereas no significant effect was observed in tumors treated with salinosporamid A alone (Fig. 4). Because angiogenesis is a key feature of tumorigenesis involved in nutrient supply and metastasis formation, we stained the tumors for CD31. Although we did not observe any difference in the density of blood vessels in the tumors, we did detect significantly reduced vessel length and diameter in the tumors treated with bortezomib and the combination ( $P < 0.001$  in all cases). Interestingly, we also observed reduced vascularity in the animals treated only with salinosporamid A ( $P < 0.001$ ) (Fig. 4). Increased levels of cleaved caspase 3 in tumors treated with bortezomib and the combination confirmed the proapoptotic effect of the proteasome inhibitors on PHEOs in mice [Figs. 3(d) and 4]. We also detected accumulation of ubiquitinated proteins in these tumors,

validating the efficient proteasome inhibition *in vivo* [Fig. 3(d)]. Again, no difference in the ubiquitin profile was observed in the animals treated with salinosporamid A, even though a significant increase in cleaved caspase 3-positive cells was seen ( $P < 0.01$ ) (Fig. 4).

The results obtained *in vivo* suggest that bortezomib alone or in combination with salinosporamid A might be a potential candidate for treatment of PHEO/PGL, as the compounds inhibit tumor cell proliferation and angiogenesis and induce cell death. In contrast, salinosporamid A is unlikely to be effective alone and may have utility only as a part of combination therapy with other proteasome inhibitors (including bortezomib) and/or other regimens and compounds used in anticancer therapies to increase the efficacy of the treatment and/or reduce the toxicity.

## Discussion

In the current study, we evaluated the effects of the proteasome inhibitors bortezomib and salinosporamid A

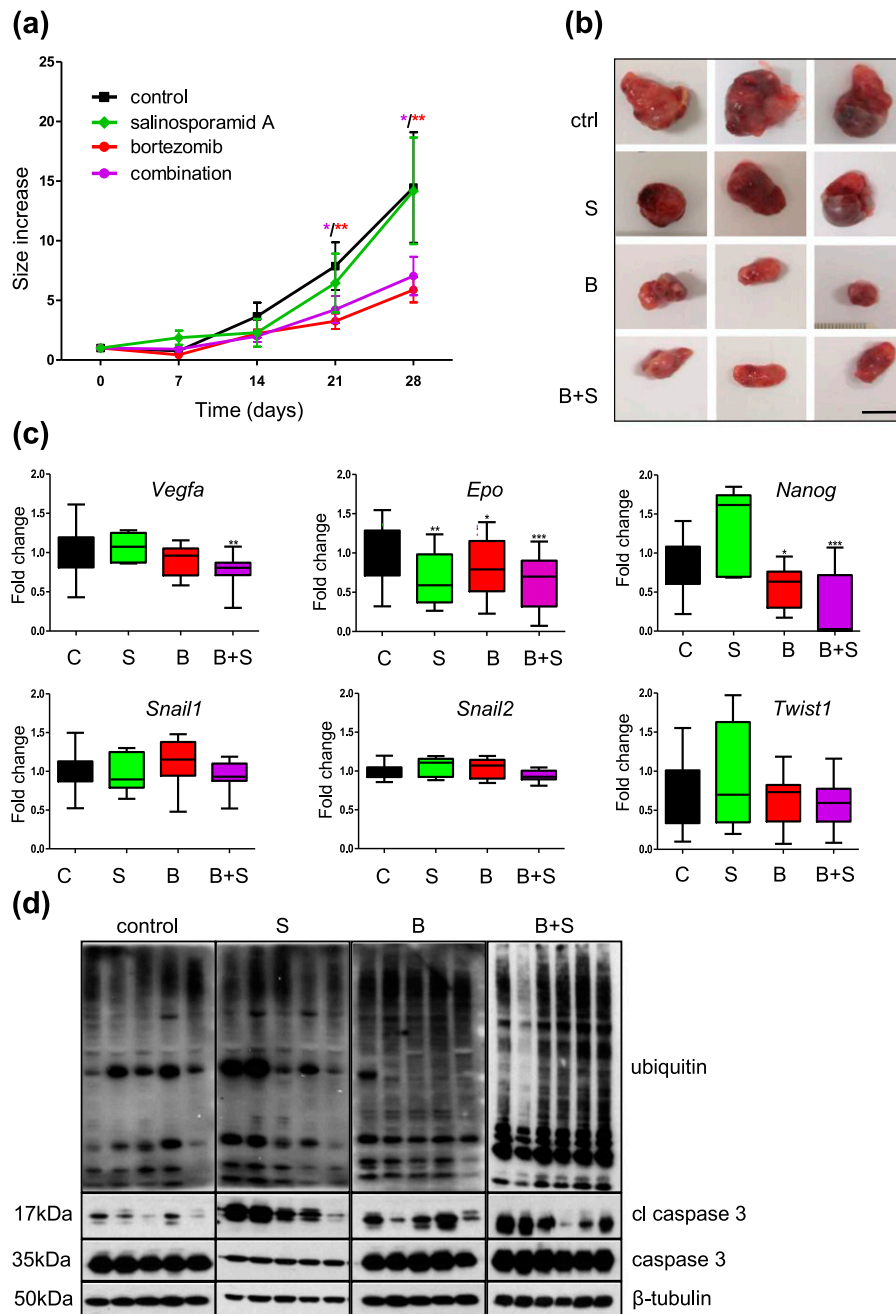


**Figure 3.** Bortezomib alone and in combination with salinosporamid A inhibits tumor growth and decreases expression levels of angiogenesis and stem cell markers *in vivo*. (a) Nude female mice bearing MTT-Luc tumors were treated with bortezomib, salinosporamid A, or a combination for 28 days. The control group was treated with vehicle. Tumor sizes were assessed once per week. The graph shows tumor growth in the groups treated with bortezomib alone (red), salinosporamid A (green), or the combination (purple) compared with control (black) animals. The graph represents data from treated and control mice assessed at specific time points as mean  $\pm$  standard error of the mean. Statistical analysis was performed by Mann–Whitney *U* test, at each time point. (b) Tumors removed from the treated and control mice after 28 days of treatment. Scale bar: 1 cm. (c) mRNA expression levels of *Vegfa*, *Epo*, *Nanog*, *Snail1*, *Snail2*, and *Twist1* in tumors from treated and control groups were assessed by quantitative real-time polymerase chain reaction. The target gene transcript levels were normalized to *Actb*. The box and whiskers graphs represent data from control ( $n = 15$ ) and treated (each group  $n = 5$ ) animals. (d) Total proteins were extracted from tumors from groups treated with bortezomib, salinosporamid A, their combination, and control animals, and were subjected to Western blot with antibodies against ubiquitin, cleaved caspase 3, and caspase 3.  $\beta$ -tubulin was used as a loading control. \* $P < 0.05$ ; \*\* $P < 0.01$ ; \*\*\* $P < 0.001$ , Mann–Whitney *U* test. B, 1 mg/kg bortezomib; B + S, combination of 0.25 mg/kg bortezomib and 0.025 mg/kg salinosporamid A; C, control; *Epo*, erythropoietin; *Nanog*, Nanog homeobox; S, 0.075 mg/kg salinosporamid A; *Snail1*, snail family zinc finger 1; *Snail2*, snail family zinc finger 2; *Vegfa*, vascular endothelial growth factor A.

in PHEO cell models *in vitro* and *in vivo*. We have shown that the cytotoxic effect of the drugs is exerted mainly via apoptosis induction. We also observed that bortezomib alone

and in combination with salinosporamid A inhibited migration and invasion of MPC *in vitro* and reduced proliferation of PHEO cancer cells and angiogenesis *in vivo*.

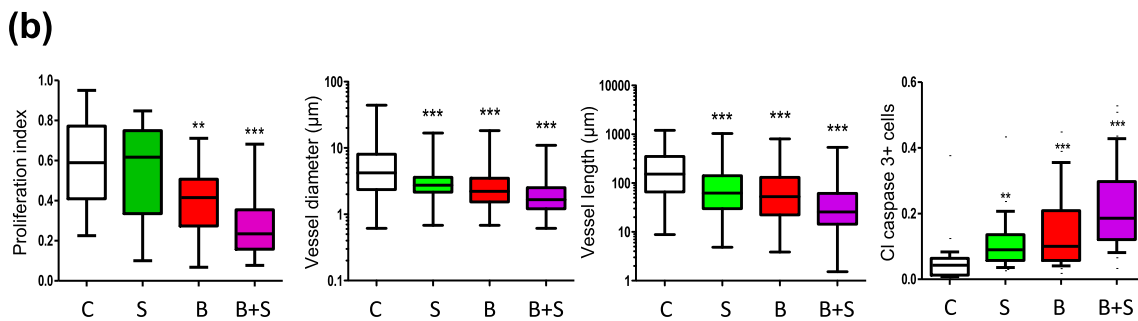
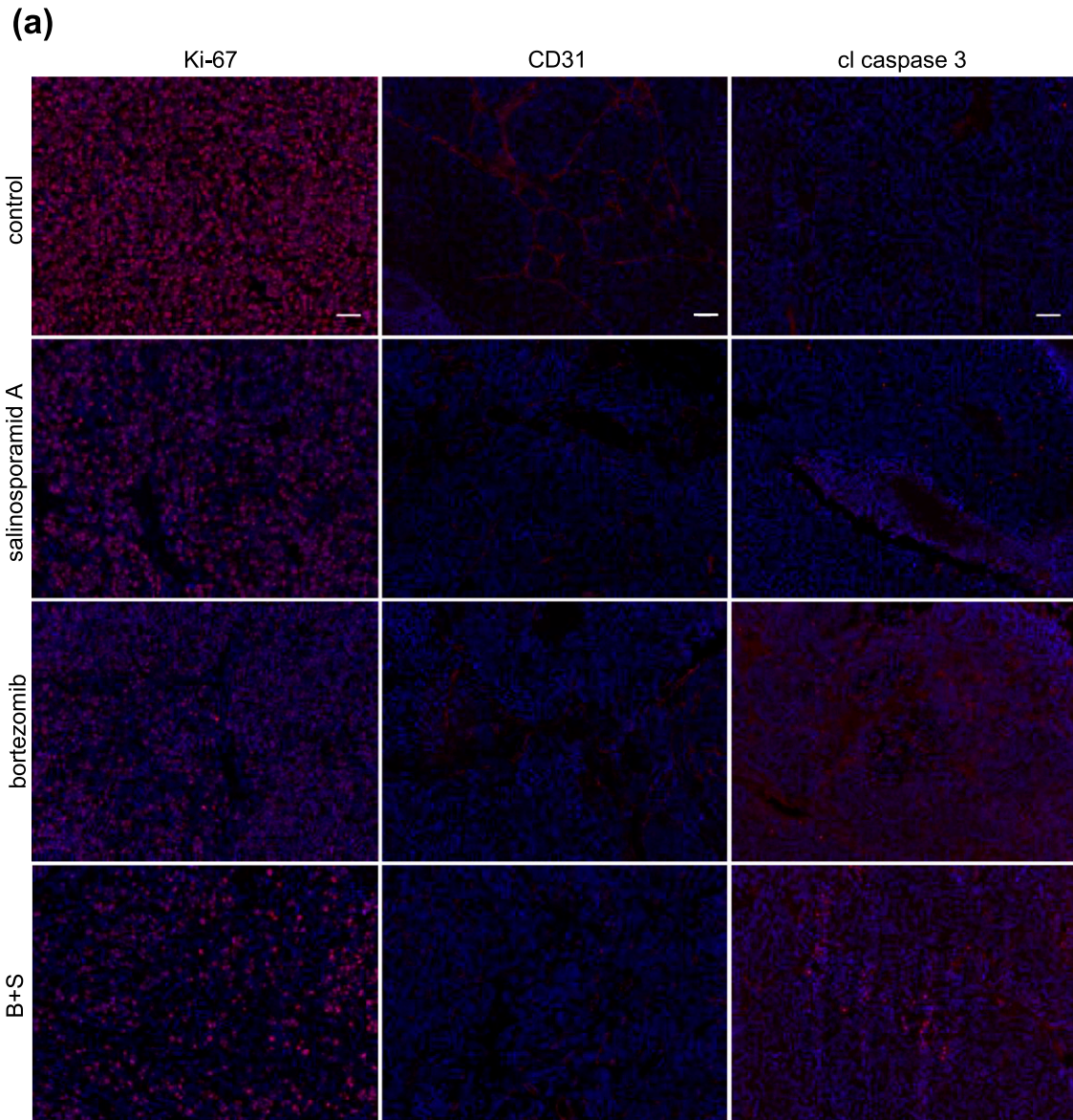


**Figure 4.** Bortezomib alone and in combination with salinosporamid A decreases tumor cell proliferation and angiogenesis and increases apoptotic cell death *in vivo*. (a) Representative images of Ki-67 staining (left), CD31 staining (middle), and cleaved caspase 3 (right) in control and treated groups (n = 5 for all groups). Proteins of interest are colored red; blue represents 4',6-diamidino-2-phenylindole staining. Magnification: ×20. Scale bar: 50 μm. (b) Box and whiskers graphs showing the proliferation index, vessel diameter, vessel length, and cleaved caspase 3–positive cells, respectively. Each graph contains data from control and treated animals (n = 5 for all groups). \*\*P < 0.01; \*\*\*P < 0.001, Mann–Whitney U test. B, 1 mg/kg bortezomib; B + S, combination of 0.25 mg/kg bortezomib and 0.025 mg/kg salinosporamid A; C, control; S: 0.075 mg/kg salinosporamid A.

Despite extensive ongoing research, metastatic PHEO/PGL remains a devastating disease with no curative treatment options besides surgery. Although the CVD

chemotherapy combination has proven to be effective in some patients, its efficacy is frequently limited by the acquisition of resistance by cancer cells (13). Therefore,

there is a need to identify effective drugs that could be used to defeat the disease or delay the occurrence of metastases after surgery. Proteasome inhibitors are emerging therapeutic compounds for various types of aggressive and highly resistant cancers (21, 22). They exert their activity by affecting several processes, including cell cycle, apoptosis, cell signaling, and transcription (3).

We decided to further investigate effects of bortezomib because the compound was previously part of a high-throughput screening study performed by our group, in which it was ranked as one of the most potent drugs to induce PHEO cell death (14). We confirmed the results in our study, in which bortezomib exerted its cytotoxicity via induction of the apoptotic pathway. This pathway is very frequently activated, either p53 dependently or independently, by this drug (5). Even though bortezomib is a very effective treatment of hematologic malignancies, it is also associated with numerous limitations, including off-target effects and short-term proteasomal inhibition (9). In initial studies, bortezomib exhibited a very high efficacy in several types of cancer cell lines; however, it has since been shown that bortezomib as a single agent is not as effective in treatment of solid tumors as it was first assumed (7, 23, 24). In contrast, salinosporamid A, which binds to all three catalytic 20S subunits irreversibly, is able to inhibit proteasome activity for a longer period of time and therefore is hypothesized to be more potent than bortezomib (8). In fact, salinosporamid A has been shown to be effective in bortezomib-refractory multiple myelomas and is in clinical trials for several types of solid tumors. In addition, fewer side effects have been associated with salinosporamid A treatment (9). It has also been reported that salinosporamid A induces apoptosis more rapidly and sustains proteasome inhibition longer than bortezomib (25). However, we did not observe the same results in MPC/MTT cell models, in which 10-fold higher concentrations of salinosporamid A than of bortezomib were necessary to activate apoptosis to a comparable extent. Similarly, when the two drugs were used at sublethal doses individually, only bortezomib had an inhibitory effect on migration and invasion of the PHEO cells. Although a study performed by Baritaki *et al.* (26) described inhibition of EMT in prostate cancer cells treated with salinosporamid A via a mechanism involving inhibition of Snail and NF- $\kappa$ B, our *in vivo* study found no significant decrease in the expression of *Snail1*, *Snail2*, and *Twist1* in tumors treated with this compound alone.

To overcome resistance development and reduce side effects of treatment, regimens affecting either the same target via slightly different mechanisms or two or more different targets are very frequently combined. Both

bortezomib and salinosporamid A have been used in combination with each other, with radio- or chemotherapy, or with other compounds, showing promising results (27–30). We combined bortezomib with salinosporamid A to decrease the bortezomib concentrations needed for treatment. In *in vitro* experiments, we showed that a combination of bortezomib and salinosporamid A activated apoptosis to a comparable level seen at a 10 times higher concentration of bortezomib alone after 24 hours. A similar effect was exhibited on EMT properties of MPC, as the combination inhibited their migration and invasion more effectively than bortezomib alone. We also observed an additive effect of the drugs in inducing death of PHEO cells, confirming previous reports demonstrating the potential of proteasome inhibitor combinations as an applicable therapeutic approach for cancer treatment (27, 31).

Our *in vivo* results are partially in accordance with the findings of Chauhan *et al.* (27), who first reported that the combination of lower doses of salinosporamid A and bortezomib inhibited tumor growth, whereas higher doses of the drugs administered individually did not. Although in their study using multiple myeloma cells neither of the two compounds exhibited a significant effect on tumor growth individually, our study found that bortezomib alone and in combination with salinosporamid A showed a similar inhibitory effect on tumor growth. In contrast, with salinosporamid A alone, no significant inhibition was observed. These results are suggestive of cell line specificity, off-target effects of bortezomib, and a different mechanism of action for inducing extended cell death independently of proteasome inhibition when compared with salinosporamid A, which has been previously reported (8). However, although the effect on tumor growth was comparable in both (bortezomib-treated and combination-treated) experimental groups, proliferation was more reduced in the tumors treated with the combination than bortezomib alone, suggesting an additive antiproliferative effect of these two drugs. It was interesting to observe that angiogenesis was inhibited in all treated animals, regardless if bortezomib, salinosporamid A, or the combination was used.

Depending on the situation, NF- $\kappa$ B exhibits either proapoptotic or antiapoptotic activity, and the NF- $\kappa$ B pathway is deregulated in numerous types of cancer (32). Although we have not evaluated inhibition of NF- $\kappa$ B signaling in this study, the results of Pacak *et al.* (33) showed that NF- $\kappa$ B inhibitors induce apoptosis in PHEO cells *in vitro* and *in vivo*. NF- $\kappa$ B suppression is thought to be the primary mechanism of action of bortezomib, as well as other proteasome inhibitors (22, 23). Proteasome inhibition suppresses NF- $\kappa$ B transcriptional activity and can thus sensitize the cells to apoptosis and regulate

metastases formation and angiogenesis via down-regulation of numerous target genes, including *VEGF* (34–36). These mechanisms were also induced by both bortezomib and salinosporamid A in PHEO cells, which suggests a prospective application of proteasome inhibitors in PHEO/PGL treatment. Bortezomib as a single agent did not show any objective response, and no remission was observed in a Phase II clinical trial in patients with metastatic carcinoids and islet cell tumors, which are also neuroendocrine tumors (37). In contrast, several reports have shown its antitumor and antiangiogenic effect on chemosensitive as well as chemoresistant neuroblastoma cell lines *in vitro* and *in vivo*, either alone or in combination with other drugs (38–41). It has also been included in Phase III of clinical trials for treatment of neuroblastoma, in which the compound is combined with a topoisomerase I inhibitor (Irinotecan), histone deacetylase inhibitor (SAHA), or an ornithine decarboxylase inhibitor (29, 42, 43). Neuroblastomas and PHEO/PGL are tumors of neuroendocrine origin, sharing numerous features. In fact, a cluster analysis performed by Szabó *et al.* (44) showed that neuroblastoma and PHEO/PGL share more similarities than any other tumors compared in the study. Despite the differences between these two types of neuroendocrine tumors, the promising findings in neuroblastoma treatment increase the probability of its efficacy also in PHEO/PGL therapy. In addition, in our previous studies, we obtained promising results using the topoisomerase I inhibitor LMP-400 and

SAHA in PHEO cells *in vitro* and *in vivo* (14, 15). Other groups also reported successful application of proteasome inhibitors in combination with heat-shock protein 90 inhibitors, which proved to be effective in PHEO cells as well (17). CVD chemotherapy is administered to patients with metastatic PHEO/PGL (13), and bortezomib has been used in combination with cyclophosphamide in several clinical trials for different types of blood cancer (45–48), suggesting the addition of bortezomib to CVD treatment might be beneficial for PHEO/PGL patients. Moreover, an increase in the stability of subunit B of succinate dehydrogenase (SDHB) via regulation of protein homeostasis represents a promising approach to rescue the function of the succinate dehydrogenase complex in PHEO/PGL (49). PHEOs/PGLs caused by mutations in *SDHB* represent the biggest challenge in the treatment of the disease, as they frequently progress toward metastatic disease. Disruption of succinate dehydrogenase function leads to a number of carcinogenesis-related processes, including increased reactive oxygen species generation and accumulation of succinate, which promotes pseudohypoxia (49). It was shown that the quantitative loss of otherwise functional mutant SDHB protein is caused by elevated ubiquitin binding and consequent proteasomal degradation. Yang *et al.* (49) showed that treatment with compounds modulating protein stability and proteostasis, including histone deacetylase inhibitors, resulted in slower degradation and decreased mutant SDHB protein ubiquitination. These results support further investigation of

## Appendix. Antibody Table

Peptide/ Protein Target	Antigen Sequence (if Known)	Name of Antibody	Manufacturer, Catalog No.	Species Raised in; Monoclonal or Polyclonal	Dilution Used	RRID
Cleaved caspase 3		Cleaved caspase-3 (Asp175) (5A1E) rabbit mAb	Cell Signaling, 9664	Rabbit; monoclonal	WB: 1:1,000; IF: 1:400	AB_2070042
Caspase 3		Caspase-3 (8G10) rabbit mAb	Cell Signaling, 9665	Rabbit; monoclonal	1:1,000	AB_2069872
Cleaved PARP		Cleaved PARP (Asp214) (7C9) mouse mAb (mouse specific)	Cell Signaling, 9548	Mouse; monoclonal	1:1,000	AB_2160592
$\beta$ -Tubulin		Monoclonal anti- $\beta$ -tubulin, clone AA2	Sigma-Aldrich, T8328	Mouse; monoclonal	1:1,000	AB_1844090
Ubiquitin		Ubiquitin antibody	Cell Signaling, 3933	Rabbit; polyclonal	1:1,000	AB_2180538
ki67		Anti-Ki67 antibody	Abcam, ab15580	Rabbit; polyclonal	1:2,000	AB_443209
CD31		Anti-CD31 antibody	Abcam, ab28364	Rabbit; polyclonal	1:50	AB_726362
Anti-mouse		Anti-mouse IgG, peroxidase-linked species-specific whole antibody (from sheep)	GE Health Care Life Sciences, NXA931	Sheep; polyclonal	1:30,000	AB_772209
Anti-rabbit		Anti-rabbit IgG, peroxidase-linked species-specific whole antibody (from donkey)	GE Health Care Life Sciences, NA934	Donkey; polyclonal	1:30,000	AB_772206
Anti-rabbit 594		DyLight 594 goat anti-rabbit IgG antibody	Vector Laboratories, DI-1594	Goat; polyclonal	1:1,000	AB_2336413

Abbreviations: IF, immunofluorescence; IgG, immunoglobulin G; mAb, monoclonal antibody; WB, Western blot.

proteasome inhibitors as future treatment options for PHEO/PGL patients, especially in combination studies.

In summary, we have shown the efficacy of bortezomib and its combination with salinosporamid A in PHEO models *in vitro* and *in vivo*. The compounds induce cell death via apoptosis, decrease PHEO cell migration and invasion, and inhibit tumor growth and cell proliferation. These findings propose that proteasome inhibitors be further investigated for their possible application in the treatment of PHEO/PGL patients. The fact that bortezomib is a Food and Drug Administration–approved drug and several other proteasome inhibitors are being tested in clinical trials makes these compounds a very attractive therapeutic option to be used either individually or, preferably, in combination with other regimens.

## Acknowledgments

We acknowledge Victoria Martucci for technical assistance in the preparation of the manuscript.

**Financial Support:** This work was supported by the Intramural Research Program of the Eunice Kennedy Shriver National Institute of Child Health and Human Development, National Institutes of Health.

**Correspondence and Reprint Requests:** Karel Pacak, MD, PhD, DSc, FACE, Eunice Kennedy Shriver National Institute of Child Health and Human Development, National Institutes of Health, Building 10, CRC, Room 1E-3140, 10 Center Drive MSC-1109, Bethesda, Maryland 20892-1109. E-mail: [karel@mail.nih.gov](mailto:karel@mail.nih.gov).

**Disclosure Summary:** The authors have nothing to disclose.

## References

- Petrelli A, Giordano S. From single- to multi-target drugs in cancer therapy: when aspecificity becomes an advantage. *Curr Med Chem*. 2008;15(5):422–432.
- Holohan C, Van Schaeybroeck S, Longley DB, Johnston PG. Cancer drug resistance: an evolving paradigm. *Nat Rev Cancer*. 2013;13(10):714–726.
- Sterz J, von Metzler I, Hahne J-C, Lamottke B, Rademacher J, Heider U, Terpos E, Sezer O. The potential of proteasome inhibitors in cancer therapy. *Expert Opin Investig Drugs*. 2008;17(6):879–895.
- Kisselev AF, van der Linden WA, Overkleeft HS. Proteasome inhibitors: an expanding army attacking a unique target. *Chem Biol*. 2012;19(1):99–115.
- Cao B, Li J, Mao X. Dissecting bortezomib: development, application, adverse effects and future direction. *Curr Pharm Des*. 2013;19(18):3190–3200.
- Selimovic D, Porzig BBOW, El-Khattouti A, Badura HE, Ahmad M, Ghanjati F, Santourlidis S, Haikel Y, Hassan M. Bortezomib/proteasome inhibitor triggers both apoptosis and autophagy-dependent pathways in melanoma cells [published correction appears in *Cell Signal*. 2015;27(3):727 and 27(5):1019–1020]. *Cell Signal*. 2013;25(1):308–318.
- Huang Z, Wu Y, Zhou X, Xu J, Zhu W, Shu Y, Liu P. Efficacy of therapy with bortezomib in solid tumors: a review based on 32 clinical trials. *Future Oncol*. 2014;10(10):1795–1807.
- Chauhan D, Catley L, Li G, Podar K, Hideshima T, Velankar M, Mitsiades C, Mitsiades N, Yasui H, Letai A, Ovaia H, Berkens C, Nicholson B, Chao TH, Neuteboom ST, Richardson P, Palladino MA, Anderson KC. A novel orally active proteasome inhibitor induces apoptosis in multiple myeloma cells with mechanisms distinct from Bortezomib. *Cancer Cell*. 2005;8(5):407–419.
- Dou QP, Zonder JA. Overview of proteasome inhibitor-based anticancer therapies: perspective on bortezomib and second generation proteasome inhibitors versus future generation inhibitors of ubiquitin-proteasome system. *Curr Cancer Drug Targets*. 2014;14(6):517–536.
- Fenical W, Jensen PR, Palladino MA, Lam KS, Lloyd GK, Potts BC. Discovery and development of the anticancer agent salinosporamide A (NPI-0052). *Bioorg Med Chem*. 2009;17(6):2175–2180.
- NCT00396864. Phase 1 clinical trial of NPI-0052 in patients with advanced solid tumor malignancies or refractory lymphoma. Available at: <https://clinicaltrials.gov/ct2/show/NCT00396864?term=NPI-0052&rank=4>. Accessed 11 October 2016.
- NCT02330562. Stage 1: marizomib + bevacizumab in WHO Gr IV GBM; stage 2: marizomib alone. Available at: <https://clinicaltrials.gov/ct2/show/NCT02330562?term=NPI-0052&rank=6>. Accessed 11 October 2016.
- Lenders JWM, Eisenhofer G. Pathophysiology and diagnosis of disorders of the adrenal medulla: focus on pheochromocytoma. *Compr Physiol*. 2014;4(2):691–713.
- Giubellino A, Shankavaram U, Bullova P, Schovaneck J, Zhang Y, Shen M, Patel N, Elkhoulou A, Lee MJ, Trepel J, Ferrer M, Pacak K. High-throughput screening for the identification of new therapeutic options for metastatic pheochromocytoma and paraganglioma. *PLoS One*. 2014;9(4):e90458.
- Schovaneck J, Bullova P, Tayem Y, Giubellino A, Wesley R, Lendvai N, Nölting S, Kopacek J, Frysak Z, Pommier Y, Kummar S, Pacak K. Inhibitory effect of the noncamptothecin topoisomerase I inhibitor LMP-400 on female mice models and human pheochromocytoma cells. *Endocrinology*. 2015;156(11):4094–4104.
- Giubellino A, Bullova P, Nölting S, Turkova H, Powers JF, Liu Q, Guichard S, Tischler AS, Grossman AB, Pacak K. Combined inhibition of mTORC1 and mTORC2 signaling pathways is a promising therapeutic option in inhibiting pheochromocytoma tumor growth: in vitro and in vivo studies in female athymic nude mice. *Endocrinology*. 2013;154(2):646–655.
- Giubellino A, Sourbier C, Lee M-J, Scroggins B, Bullova P, Landau M, Ying W, Neckers L, Trepel JB, Pacak K. Targeting heat shock protein 90 for the treatment of malignant pheochromocytoma. *PLoS One*. 2013;8(2):e56083.
- Matro J, Giubellino A, Pacak K. Current and future therapeutic approaches for metastatic pheochromocytoma and paraganglioma: focus on SDHB tumors. *Horm Metab Res*. 2013;45(2):147–153.
- Korpershoek E, Pacak K, Martiniova L. Murine models and cell lines for the investigation of pheochromocytoma: applications for future therapies? *Endocr Pathol*. 2012;23(1):43–54.
- Schindelin J, Arganda-Carreras I, Frise E, Kaynig V, Longair M, Pietzsch T, Preibisch S, Rueden C, Saalfeld S, Schmid B, Tinevez JY, White DJ, Hartenstein V, Eliceiri K, Tomancak P, Cardona A. Fiji: an open-source platform for biological-image analysis. *Nat Methods*. 2012;9(7):676–682.
- Hideshima T, Richardson P, Chauhan D, Palombella VJ, Elliott PJ, Adams J, Anderson KC. The proteasome inhibitor PS-341 inhibits growth, induces apoptosis, and overcomes drug resistance in human multiple myeloma cells. *Cancer Res*. 2001;61(7):3071–3076.
- Almond JB, Cohen GM. The proteasome: a novel target for cancer chemotherapy. *Leukemia*. 2002;16(4):433–443.
- Adams J, Palombella VJ, Sausville EA, Johnson J, Destree A, Lazarus DD, Maas J, Pien CS, Prakash S, Elliott PJ. Proteasome inhibitors: a novel class of potent and effective antitumor agents. *Cancer Res*. 1999;59(11):2615–2622.
- Caravita T, de Fabritiis P, Palumbo A, Amadori S, Boccadoro M. Bortezomib: efficacy comparisons in solid tumors and hematologic malignancies. *Nat Clin Pract Oncol*. 2006;3(7):374–387.

25. Ruiz S, Krupnik Y, Keating M, Chandra J, Palladino M, McConkey D. The proteasome inhibitor NPI-0052 is a more effective inducer of apoptosis than bortezomib in lymphocytes from patients with chronic lymphocytic leukemia. *Mol Cancer Ther.* 2006;5(7):1836–1843.
26. Baritaki S, Chapman A, Yeung K, Spandidos DA, Palladino M, Bonavida B. Inhibition of epithelial to mesenchymal transition in metastatic prostate cancer cells by the novel proteasome inhibitor, NPI-0052: pivotal roles of Snail repression and RKIP induction. *Oncogene.* 2009;28(40):3573–3585.
27. Chauhan D, Singh A, Brahmandam M, Podar K, Hideshima T, Richardson P, Munshi N, Palladino MA, Anderson KC. Combination of proteasome inhibitors bortezomib and NPI-0052 trigger in vivo synergistic cytotoxicity in multiple myeloma. *Blood.* 2008;111(3):1654–1664.
28. Gatti L, Zuco V, Zaffaroni N, Perego P. Drug combinations with proteasome inhibitors in antitumor therapy. *Curr Pharm Des.* 2013;19(22):4094–4114.
29. NCT00644696. Study of irinotecan and bortezomib in children with recurrent/refractory neuroblastoma. Available at: <https://clinicaltrials.gov/ct2/show/NCT00644696?term=bortezomib&rank=3>. Accessed 11 October 2016.
30. NCT02903069. Study of marizomib with temozolomide and radiotherapy in patients with newly diagnosed brain cancer. Available at: <https://clinicaltrials.gov/ct2/show/NCT02903069?term=NPI-0052&rank=7>. Accessed 2 May 2017.
31. Shirley RB, Kaddour-Djebbar I, Patel DM, Lakshmiathan V, Lewis RW, Kumar MV. Combination of proteasomal inhibitors lactacystin and MG132 induced synergistic apoptosis in prostate cancer cells. *Neoplasia.* 2005;7(12):1104–1111.
32. Zerbini LF, Libermann TA. Life and death in cancer: GADD45 alpha and gamma are critical regulators of NF-kappaB mediated escape from programmed cell death. *Cell Cycle.* 2005;4(1):18–20.
33. Pacak K, Sirova M, Giubellino A, Lencesova L, Csaderova L, Laukova M, Hudecova S, Krizanova O. NF- $\kappa$ B inhibition significantly upregulates the norepinephrine transporter system, causes apoptosis in pheochromocytoma cell lines and prevents metastasis in an animal model. *Int J Cancer.* 2012;131(10):2445–2455.
34. Daniel KG, Kuhn DJ, Kazi A, Dou QP. Anti-angiogenic and anti-tumor properties of proteasome inhibitors. *Curr Cancer Drug Targets.* 2005;5(7):529–541.
35. Oikawa T, Sasaki T, Nakamura M, Shimamura M, Tanahashi N, Omura S, Tanaka K. The proteasome is involved in angiogenesis. *Biochem Biophys Res Commun.* 1998;246(1):243–248.
36. Politou M, Naresh K, Terpos E, Crawley D, Lampert I, Apperley JF, Rahemtulla A. Anti-angiogenic effect of bortezomib in patients with multiple myeloma. *Acta Haematol.* 2005;114(3):170–173.
37. Shah MH, Young D, Kindler HL, Webb I, Kleiber B, Wright J, Grever M. Phase II study of the proteasome inhibitor bortezomib (PS-341) in patients with metastatic neuroendocrine tumors. *Clin Cancer Res.* 2004;10(18 Pt 1):6111–6118.
38. Armstrong MB, Schumacher KR, Mody R, Yanik GA, Opiari AW, Jr, Castle VP. Bortezomib as a therapeutic candidate for neuroblastoma. *J Exp Ther Oncol.* 2008;7(2):135–145.
39. Michaelis M, Fichtner I, Behrens D, Haider W, Rothweiler F, Mack A, Cinatl J, Doerr HW, Cinatl J, Jr. Anti-cancer effects of bortezomib against chemoresistant neuroblastoma cell lines in vitro and in vivo. *Int J Oncol.* 2006;28(2):439–446.
40. Pagnan G, Di Paolo D, Carosio R, Pastorino F, Marimpietri D, Brignole C, Pezzolo A, Loi M, Galiotta LJ, Piccardi F, Cilli M, Nico B, Ribatti D, Pistoia V, Ponzoni M. The combined therapeutic effects of bortezomib and fenretinide on neuroblastoma cells involve endoplasmic reticulum stress response. *Clin Cancer Res.* 2009;15(4):1199–1209.
41. Hamner JB, Dickson PV, Sims TL, Zhou J, Spence Y, Ng CY, Davidoff AM. Bortezomib inhibits angiogenesis and reduces tumor burden in a murine model of neuroblastoma. *Surgery.* 2007;142(2):185–191.
42. NCT01132911. A Phase I study of vorinostat and bortezomib in children with refractory of recurrent solid tumors, including CNS tumors and lymphomas. Available at: <https://clinicaltrials.gov/ct2/show/NCT01132911?term=bortezomib+neuroblastoma&rank=4>. Accessed 2 May 2017.
43. NCT02139397. Study of DFMO in combination with bortezomib for relapsed or refractory neuroblastoma. Available at: <https://clinicaltrials.gov/ct2/show/NCT02139397?term=bortezomib+neuroblastoma&rank=2>. Accessed 11 October 2016.
44. Szabó PM, Pintér M, Szabó DR, Zsippai A, Patócs A, Falus A, Rácz K, Igaz P. Integrative analysis of neuroblastoma and pheochromocytoma genomics data. *BMC Med Genomics.* 2012;5:48.
45. NCT00833560. Clinical study on induction of remission using bortezomib (Vel), cyclophosphamide (C), and dexamethasone (D) in patients until 60 years of age with untreated multiple myeloma and planned for a high dose chemotherapy: (VelCD; Deutsche Studiengruppe Multiples Myelom [DSMM] XIa). Available at: <https://clinicaltrials.gov/ct2/show/study/NCT00833560?term=bortezomib+cyclophosphamide&recrs=de&phase=12&draw=2&rank=1>. Accessed 31 July 2017.
46. NCT02467010. Bortezomib in combination with continuous low-dose oral cyclophosphamide and dexamethason followed by maintenance in primary refractory or relapsed bortezomib naive multiple myeloma patients: a prospective phase II study. Available at: <https://clinicaltrials.gov/ct2/show/study/NCT02467010?term=bortezomib+cyclophosphamide&recrs=de&phase=12&draw=2&rank=2>. Accessed 31 July 2017.
47. NCT00722137. A randomized, open-label, multicentre phase 3 study of the combination of rituximab, cyclophosphamide, doxorubicin, VELCADE, and prednisone or rituximab, cyclophosphamide, doxorubicin, vincristine, and prednisone in patients with newly diagnosed mantle cell lymphoma who are not eligible for a bone marrow transplant. Available at: <https://clinicaltrials.gov/ct2/show/NCT00722137?term=NCT00722137&rank=1>. Accessed 31 July 2017.
48. NCT00958256. Phase II study of bortezomib in combination with cyclophosphamide and rituximab for relapsed/refractory mantle cell lymphoma. Available at: <https://clinicaltrials.gov/ct2/show/NCT00958256?term=NCT00958256&rank=1>. Accessed 31 July 2017.
49. Yang C, Matro JC, Huntoon KM, Ye DY, Huynh TT, Fliedner SMJ, Breza J, Zhuang Z, Pacak K. Missense mutations in the human SDHB gene increase protein degradation without altering intrinsic enzymatic function. *FASEB J.* 2012;26(11):4506–4516.